

Antiferromagnetic fluctuations and a dominant d_{xy} -wave pairing symmetry in nickelate-based superconductors

Chao Chen,¹ Runyu Ma,¹ Xuelei Sui,² Ying Liang,¹ Bing Huang,^{2,1} and Tianxing Ma^{1,2,*}

¹*Department of Physics, Beijing Normal University, Beijing 100875, China*

²*Beijing Computational Science Research Center, Beijing 100084, China*

Motivated by recent experimental studies that superconductivity found in nickelate-based materials, we study the temperature dependence of the spin correlation and the superconducting pairing interaction within an effective two-band Hubbard model by quantum Monte Carlo method. Our intensive numerical results reveal that the pairing with a d_{xy} -wave symmetry firmly dominates over other pairings at low temperature. It is also found that the (π, π) antiferromagnetic correlation and the effective pairing interaction are both enhanced as the on-site Coulomb interaction increases, demonstrating that the superconductivity is driven by strong electron-electron correlation. Our work shares an exact numerical results to understand the superconducting mechanism of nickelate-based materials.

Introduction Understanding the mechanism of high-Tc superconductivity has always been a central issue in condensed matter physics[1–7]. Recently, the discovery of superconductivity in the family of Sr-doped RNiO_2 ($\text{R}=\text{Nd}, \text{La}$) has attracted great research interests, which may provide a new opportunity for further understanding unconventional superconductivity[8–23]. Among them, one essential object is to identify the dominant superconducting pairing form, which remains as a major challenge of today’s studies on this family. In a single particle tunneling experiment on Sr-doped NdNiO_2 film surface, researchers detected singlet pairing but they cannot distinguish whether it is s -wave or d -wave or their mixture[24]. At present, some theoretical studies of nickelate-based superconductors are based on models with one-orbital ($\text{Ni } 3d$) band structures which support these materials can be captured by a one-band Hubbard model[25, 26], and they get a dominant d -wave pairing in their model[25, 26]. While, others propose various possibility of multiband model[27–31]. The $t - J - K$ model which consider the Kondo coupling, exists a transition between d -wave and $(d+is)$ -wave of the dominant pairing at large hole doping[32]. Research on the controversial pair symmetry of nickelate is necessary both experimentally and theoretically. From the viewpoint of theory, using unbiased numerical techniques is believed to be the only opportunity to win this great challenge if the electronic correlation dominates in the system.

Previous theoretical works by density-functional theory (DFT)[10, 33–36] have studied the characteristics of the nickelate’s electronic structure. It was found that there were both similarities and differences, compared with that of cuprates[10, 28, 30, 35–39]. These results provided a good background to study the magnetism and superconductivity in nickelate’s family. According to the calculation of DFT on RNiO_2 [10, 35, 36], the two bands near the E_F mainly contributed to its physical properties. One band, composed of $\text{Ni } 3d_{x^2-y^2}$ and $\text{O } 2p$ orbitals, has a Zhang-Rice-singlet-like character, while

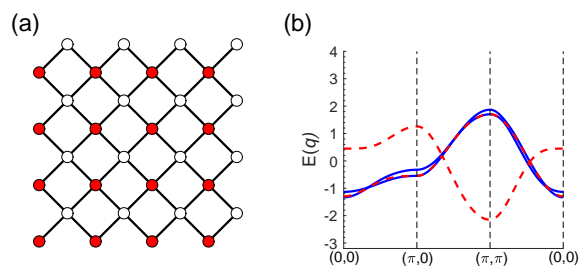


FIG. 1. (Color online)(a) Here red and white circles indicate different sublattice, A and B. (b) The energy band along high symmetry line in unfolded Brillouin Zone. Solid blue lines: $k_z=0$; dashed red lines: $k_z = \pi$ in Table.I.

the contribution of oxygen in the nickelate is smaller than that in cuprates, and the other band, composed of $\text{R } 5d$ orbitals, forms an important metallic electron pocket. These two orbitals hybridize, forming a system, where the strongly correlated Ni layers plays an important role[10, 35, 36].

To identify the superconducting pairing form of nickelate-based materials, we perform a quantum Monte Carlo study of the spin correlation and superconducting pairing interaction in an effective two-band microscopic model. From results of the Wannier orbitals[10, 35], a two-band model is constructed which contains two main bands near E_F , and this model also contains inter-orbital coupling between the $\text{Ni } 3d$ orbital and the $\text{R } 5d$ orbital. The calculations of the pairing correlation shows that there exists an extensive d -wave channel which firmly dominates over other pairings at low temperature. For different fillings $\langle n \rangle = 1.0, 0.9, 0.8$, the (π, π) antiferromagnetic (AFM) correlation and the effective pairing interaction are both enhanced as the on-site Coulomb interaction increases. Our unbiased calculations demonstrate that the superconductivity and AFM correlation in nickelate-based superconductors should be driven by electron-electron correlation, and our

Hopping parameters for the tight binding model			
k_z	0	$\pi/2$	π
t^{Nd}			
Δ_1	0.633	1.305	1.977
t_1	-0.380	-0.028	0.324
t_2	0.084	-0.090	-0.264
t_3	0.003	0.027	0.051
t^{Ni}			
Δ_2	0.242	0.308	0.374
t_1	-0.374	-0.374	-0.374
t_2	0.094	0.094	0.094
t_3	-0.043	-0.043	-0.043
t^{Nd-Ni}			
t_3	0.002	0.002	0.002

TABLE I. Hopping parameters for the tight binding model from Refs.[10, 35, 36].

work here marks an important step in an exact manner to address the superconducting mechanism in nickelate's family.

Model and methods In the extended two-band Hubbard model, the tight-binding part contains the intralayer hoppings, the interlayer hoppings and the strongly correlated Ni layer. Therefore, the nickel-square lattice Hamiltonian can be written as

$$\begin{aligned}
H &= H_1 + H_2 + H_3 + H_4, \\
H_1 &= t_3^{Nd-Ni} \sum_{i\eta\sigma} [a_{i\sigma}^\dagger b_{i+\eta\sigma} + h.c.], \\
H_2 &= t_1^{Nd} [\sum_{i\tau_1\sigma} a_{i\sigma}^\dagger a_{i+\tau_1\sigma}] + t_2^{Nd} [\sum_{i\tau_2\sigma} a_{i\sigma}^\dagger a_{i+\tau_2\sigma}] \\
&\quad + t_3^{Nd} [\sum_{i\tau_3\sigma} a_{i\sigma}^\dagger a_{i+\tau_3\sigma}], \\
H_3 &= t_1^{Ni} [\sum_{i\tau_1\sigma} b_{i\sigma}^\dagger b_{i+\tau_1\sigma}] + t_2^{Ni} [\sum_{i\tau_2\sigma} b_{i\sigma}^\dagger b_{i+\tau_2\sigma}] \\
&\quad + t_3^{Ni} [\sum_{i\tau_3\sigma} b_{i\sigma}^\dagger b_{i+\tau_3\sigma}], \\
H_4 &= U \sum_i n_{bi\uparrow} n_{bi\downarrow} + \mu \sum_{i\sigma} [(1 + \Delta/\mu) n_{ai\sigma} + n_{bi\sigma}] \quad (1)
\end{aligned}$$

Here, $a_{i\sigma}$ ($a_{i\sigma}^\dagger$) annihilates (creates) electrons at site \mathbf{R}_i with spin σ ($\sigma=\uparrow, \downarrow$) on sublattice A, $b_{i\sigma}$ ($b_{i\sigma}^\dagger$) annihilates (creates) electrons at the site \mathbf{R}_i with spin σ ($\sigma=\uparrow, \downarrow$) on sublattice B, $n_{ai\sigma} = a_{i\sigma}^\dagger a_{i\sigma}$, $n_{bi\sigma} = b_{i\sigma}^\dagger b_{i\sigma}$, $\eta = (\pm 3\hat{x}, \pm 3\hat{y})$, and $\tau_1 = (\pm 2\hat{x}, 0)$ and $(0, \pm 2\hat{y})$, and $\tau_2 = (\pm 2\hat{x}, \pm 2\hat{y})$, and $\tau_3 = (\pm 4\hat{x}, 0)$ and $(0, \pm 4\hat{y})$. Our first-principles calculations are basically consistent with the data in the Refs.[10, 35, 36]. More details about our wannier downfolding of NdNiO₂, please see the table in Appdenix. For simplicity and clarity, we mainly take the parameters from Refs.[10, 35, 36], and

list the hopping parameters of NdNiO₂ in Table.I at $k_z=0$, $\pi/2$ and π . From analysis of the first-principles calculations[10, 35, 36, 40, 41], here $\Delta=\Delta_1-\Delta_2$ represents the on-site energy difference between the Nd 5d orbital and the Ni 3d orbital. In the following calculations, we mainly discuss the cases of $k_z=0$ and $k_z=\pi$.

Our simulations are mainly performed on lattice shown in Fig.1 (a) of $L=8$ (the total number of lattice sites is $N_s=2\times L^2=128$) by using determinant quantum Monte Carlo (DQMC) method at finite temperature with periodic boundary conditions. The basic strategy of the DQMC method is to express the partition function as a high-dimensional integrals on a set of random auxiliary fields. Then the Monte Carlo techniques completes the integral. In the simulations, we use 3000 sweeps to equilibrate the system, and an additional 10000 sweeps to generate measurements. These measurements were split into 10 bins and provided the basis of coarse-grain averages. The errors were calculated based on the standard deviation from the average. For more technical details, please see Refs.[42–44].

As magnetic excitation possibly plays a significant role in superconductivity mechanism of electronic correlated systems, we investigate the spin susceptibility in the z direction at zero frequency,

$$\chi(q) = \int_0^\beta d\tau \sum_{d,d'=a,b} \sum_{\mathbf{i},\mathbf{j}} e^{iq\cdot(\mathbf{i}_d - \mathbf{j}_{d'})} \langle \mathbf{m}_{\mathbf{i}_d}(\tau) \cdot \mathbf{m}_{\mathbf{j}_{d'}}(0) \rangle, \quad (2)$$

where $m_{\mathbf{i}_a}(\tau) = e^{H\tau} m_{\mathbf{i}_a}(0) e^{-H\tau}$ with $m_{\mathbf{i}_a} = a_{i\uparrow}^\dagger a_{i\uparrow} - a_{i\downarrow}^\dagger a_{i\downarrow}$ and $m_{\mathbf{i}_b} = b_{i\uparrow}^\dagger b_{i\uparrow} - b_{i\downarrow}^\dagger b_{i\downarrow}$. In order to study the superconducting property of nickelate-based superconductors, we calculated the pairing susceptibility,

$$P_\alpha = \frac{1}{N_s} \sum_{\mathbf{i},\mathbf{j}} \int_0^\beta d\tau \langle \Delta_\alpha^\dagger(\mathbf{i}, \tau) \Delta_\alpha(\mathbf{j}, 0) \rangle, \quad (3)$$

where α denotes the pairing symmetry. Due to the constraint of different on-site Hubbard interaction in two sublattices, pairing between the same sublattices is favored and the corresponding order parameter $\Delta_\alpha^\dagger(\mathbf{i})$ is written as

$$\Delta_\alpha^\dagger(\mathbf{i}) = \sum_l f_\alpha(\delta_l) (a_{i\uparrow}^\dagger b_{i+\delta_l\downarrow} - a_{i\downarrow}^\dagger b_{i+\delta_l\uparrow})^\dagger,$$

where $f_\alpha(\delta_l)$ stands for the form factor of pairing function. The vectors δ_l ($l=1,2,3,4$) represent the nearest inter-sublattice connections, where δ is $(\pm\hat{x}, \pm\hat{y})$, or the nearest intra-sublattice connections where δ' is $(\pm 2\hat{x}, 0)$ and $(0, \pm 2\hat{y})$.

We referenced four kinds of pairing form from iron-square lattice[44], which was pictured in Fig.2. These

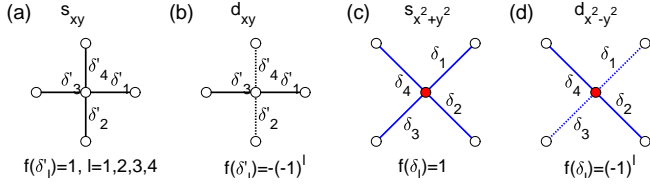


FIG. 2. (Color online) Phase of the s_{xy} , d_{xy} , $s_{x^2+y^2}$ and $d_{x^2-y^2}$.

singlet s -wave and d -wave pairing have the form factor,

$$\begin{aligned} s_{xy}\text{-wave} &: f_{s_{xy}}(\delta'_l) = 1, \quad l = 1, 2, 3, 4, \\ d_{xy}\text{-wave} &: f_{d_{xy}}(\delta'_l) = 1 (\delta'_l = (\pm 2\hat{x}, 0)), \\ \text{and} & \quad f_{d_{xy}}(\delta'_l) = -1 (\delta'_l = (0, \pm 2\hat{y})), \\ s_{x^2+y^2}\text{-wave} &: f_{s_{x^2+y^2}}(\delta'_l) = 1, \quad l = 1, 2, 3, 4, \\ d_{x^2-y^2}\text{-wave} &: f_{d_{x^2-y^2}}(\delta'_l) = 1 (\delta'_l = \pm(-\hat{x}, \hat{y})) \\ \text{and} & \quad f_{d_{x^2-y^2}}(\delta'_l) = -1 (\delta'_l = \pm(\hat{x}, \hat{y})). \end{aligned} \quad (4)$$

Results and discussion In order to study the magnetic correlations, we calculated the spin susceptibility $\chi(\mathbf{q})$ in Fig.3 at different U and fillings $\langle n \rangle$ at temperature $T=1/6$. From Fig.3(a) and Fig.3(b), one can notice that there is a smooth peak at (π, π) which indicating the existence of AFM correlation at $k_z = 0$. In Fig.3 (a), we can see that the AFM correlation is enhanced as U increases, which indicates that such an AFM correlation is driven by strong electron-electron correlation. Fig.3 (b) shows that the peak is almost identical at different fillings, which indicates that the AFM correlation is nearly unchanged when the system is doped away from half filling. However, from Fig.3(c) and Fig.3(d) at $k_z = \pi$, we can see a small transition from FM to AFM as the filling decreases from 1.0. Recently, resonant inelastic X-ray scattering experiment revealed that there exit an AFM exchange interaction[45]. Our results here might provide an evidence for the AFM exchange couplings that observed in nickelate-based superconductors.

In Fig. 4(a) we show the temperature dependence of pairing susceptibilities for different pairing symmetries at half filling with $U=1.122$ at $k_z = 0$. We can clearly notice that the pairing susceptibilities for various pairing symmetries increase with the lowering of temperature. Most strikingly, d_{xy} increases much faster than any other pairings symmetry as the temperature is lowered. This indicates that the d_{xy} pairing symmetry is dominant over the other pairing symmetry at half filling. Our further results also illustrate that the d_{xy} pairing symmetry is robust at different fillings and U .

The effective pairing interaction is a direct probe for the superconductivity. To extract the effective pairing interaction, the uncorrelated single-particle contribution $\tilde{P}_\alpha(\mathbf{i}, \mathbf{j})$ is calculated, which is achieved by replacing $\langle a_{\mathbf{i}\downarrow}^\dagger b_{\mathbf{j}\uparrow}^\dagger a_{\mathbf{i}+\delta_l\downarrow}^\dagger b_{\mathbf{j}+\delta_l\uparrow} \rangle$ in Eq. 3 with $\langle a_{\mathbf{i}\downarrow}^\dagger b_{\mathbf{j}\uparrow}^\dagger \rangle \langle a_{\mathbf{i}+\delta_l\downarrow}^\dagger b_{\mathbf{j}+\delta_l\uparrow} \rangle$,

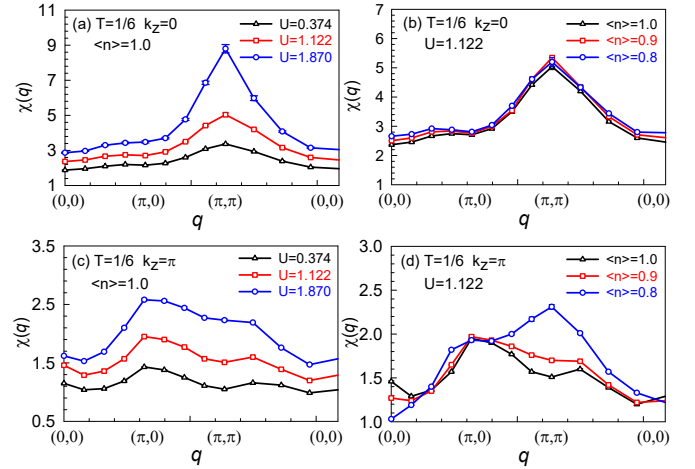


FIG. 3. (Color online) (a) Magnetic susceptibility $\chi(q)$ versus momentum q for different U at $\langle n \rangle = 1.0$ and $k_z = 0$ on a 2×8^2 lattice. (b) Magnetic susceptibility $\chi(q)$ versus momentum q for different fillings at $U = 1.122$ and $k_z = 0$ on a 2×8^2 lattice. (c) Magnetic susceptibility $\chi(q)$ versus momentum q for different U at $\langle n \rangle = 1.0$ and $k_z = \pi$ on a 2×8^2 lattice. (d) Magnetic susceptibility $\chi(q)$ versus momentum q for different fillings at $U = 1.122$ and $k_z = \pi$ on a 2×8^2 lattice.

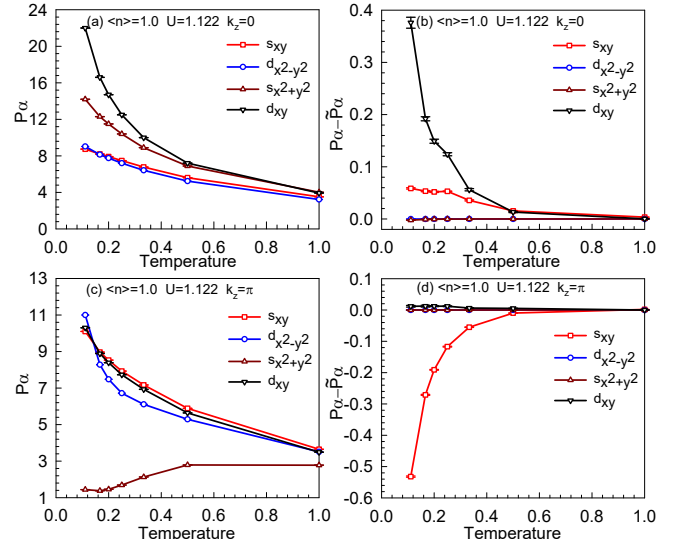


FIG. 4. (Color online) (a) Pairing susceptibility P_α as a function of temperature for different pairing symmetries at $\langle n \rangle = 1.0$, $U = 1.122$ and $k_z = 0$ on a 2×8^2 lattice. (b) The effective pairing interaction $P_\alpha - \tilde{P}_\alpha$ as a function of temperature for different pairing symmetries at $\langle n \rangle = 1.0$, $U = 1.122$, $k_z = 0$ on a 2×8^2 lattice. (c) Pairing susceptibility P_α as a function of temperature for different pairing symmetries at $\langle n \rangle = 1.0$, $U = 1.122$ and $k_z = \pi$ on a 2×8^2 lattice. (d) The effective pairing interaction $P_\alpha - \tilde{P}_\alpha$ as a function of temperature for different pairing symmetries at $\langle n \rangle = 1.0$, $U = 1.122$, $k_z = \pi$ on a 2×8^2 lattice.

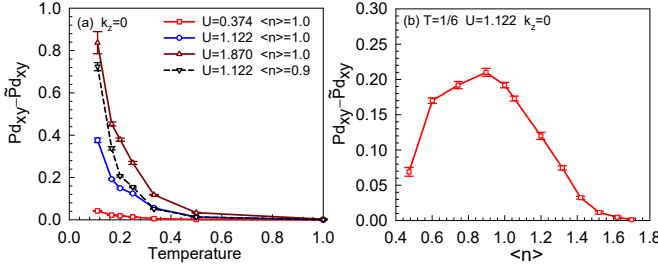


FIG. 5. (Color online) (a) The effective paring interaction $P_{d_{xy}} - \tilde{P}_{d_{xy}}$ as a function of temperature for different U at $\langle n \rangle = 1.0$ and $k_z = 0$ on a 2×8^2 lattice. (b) The effective paring interaction $P_{d_{xy}} - \tilde{P}_{d_{xy}}$ as a function of fillings at $T = 1/6$, $U = 1.122$ and $k_z = 0$ on a 2×8^2 lattice.

and then we get the effective pairing interaction $P_\alpha - \tilde{P}_\alpha$. In Fig. 4(b), it is obvious that $P_\alpha - \tilde{P}_\alpha$ presents a very similar temperature dependence to that of P_α . Moreover, the effective pairing interaction for d_{xy} pairing, is always positive and increases much faster than any other pairings symmetry at low temperatures. Such a temperature dependence shows that there indeed exists attraction for the d_{xy} pairing at $k_z = 0$. From Fig. 4(c) and Fig. 4(d), we can't find a pairing symmetry always increase at low temperatures and the effective pairing interaction for all pairing symmetry are very small. Therefore, with the hopping parameter $t_i^N d$ changed, the investigated effective pairing interaction with the four pairings symmetry might disappear. In the following, we mainly discuss the hopping parameter for $k_z = 0$.

Fig. 5(a) shows the effective pairing interaction as a function of temperature for d_{xy} wave at different U . We can see that the effective pairing interaction of d_{xy} wave is enhanced with the increasing of U . For $U=0.374$, the effective pairing interaction $P_{d_{xy}} - \tilde{P}_{d_{xy}}$ is very small even in low temperature region, this may due to the small AFM structure of the system in Fig. 3(a). For $U=1.122$ and $U=1.870$, remarkably, the effective pairing interaction $P_{d_{xy}} - \tilde{P}_{d_{xy}}$ tends to diverge in low temperatures, and with the increasing of U this diverge tends to be promoted. This indicates that the d_{xy} pairing superconductivity should be driven by strong electron-electron correlation.

In Fig. 5(b), we studied the filling dependence of effective pairing interaction $P_{d_{xy}} - \tilde{P}_{d_{xy}}$ at $T = 1/6$, $U = 1.122$ and $k_z = 0$. Fig. 5 (b) indicates that the effective paring interaction $P_{d_{xy}} - \tilde{P}_{d_{xy}}$ is the largest around filling 0.9. As that shown in Fig. 3 and Fig. 5, the increase of the peak at (π, π) of spin susceptibility is correlated with the promoting of the pairing susceptibility. This directly confirms that the (π, π) AFM fluctuations enhance the d_{xy} pairing.

In summary, within an effective two-band model for nickelate-based superconductors, we study the spin correlation and the superconducting pairing interaction

by using the unbiased numerical techniques of DQMC. We identify that the d_{xy} wave paring channel to be dominant in nickelate-based superconductors. Both the (π, π) AFM and the paring susceptibility of d_{xy} symmetry are enhanced with the increasing of electron-electron correlation, especially in low temperature region. Moreover, as the electronic filling decreases from half filling, the paring susceptibility of d_{xy} symmetry is also enhanced around $\langle n \rangle = 0.9$. The calculated AFM, the behavior of pairing susceptibility and effective pairing interaction might support the microscopic superconducting mechanism for cuprates and nickelate-based superconductors is identical.

Acknowledgement — We thank Huijia Dai and Jingyao Meng for useful discussion. This work was supported by NSFC (Nos. 11974049). The numerical simulations in this work were performed at HSCL of Beijing Normal University and Tianhe in Beijing Computational Science Research Center.

Appendix

In consideration of the two band model in our Hamiltonian, we chose orbital sets of $Ni_{3d_{x^2-y^2}}$ and $Nd/La_{5d_{z^2}}$ in Wannier downfolding calculations as implemented in Wannier90[46], which can reproduce the band structure near the Fermi level accurately. The calculated hopping parameters for two-orbital wannierization are listed in Table. II(c)

-
- * txma@bnu.edu.cn
- [1] J. Bardeen, L. N. Cooper, and J. R. Schrieffer, *Phys. Rev.* **108**, 1175 (1957).
 - [2] J. G. Bednorz and K. A. Müller, *Zeitschrift für Physik B Condensed Matter* **64**, 189 (1986).
 - [3] P. W. Anderson, *Science* **235**, 1196 (1987).
 - [4] J. G. Bednorz and K. A. Müller, *Rev. Mod. Phys.* **60**, 585 (1988).
 - [5] P. W. Anderson, P. A. Lee, M. Randeria, T. M. Rice, N. Trivedi, and F. C. Zhang, *Journal of Physics: Condensed Matter* **16**, R755 (2004).
 - [6] P. A. Lee, N. Nagaosa, and X.-G. Wen, *Rev. Mod. Phys.* **78**, 17 (2006).
 - [7] D. J. Scalapino, *Rev. Mod. Phys.* **84**, 1383 (2012).
 - [8] D. Li, K. Lee, B. Y. Wang, M. Osada, S. Crossley, H. R. Lee, Y. Cui, Y. Hikita, and H. Y. Hwang, *Nature* **572**, 624 (2019).
 - [9] G. A. Sawatzky, *NATURE* **572**, 592 (AUG 29).
 - [10] M. Hepting, D. Li, C. J. Jia, H. Lu, E. Paris, Y. Tseng, X. Feng, M. Osada, E. Been, Y. Hikita, Y.-D. Chuang, Z. Hussain, K. J. Zhou, A. Nag, M. Garcia-Fernandez, M. Rossi, H. Y. Huang, D. J. Huang, Z. X. Shen, T. Schmitt, H. Y. Hwang, B. Moritz, J. Zaanen, T. P. Devereaux, and W. S. Lee, *Nature Materials* **19**, 381 (2020).

Hopping parameters for the tight binding model					
			$NdNiO^2$	$LaNiO^2$	
i	j	k	$t_{[i,j,k]}^{Nd}$		
0	0	0	0.268885	0.106574	
1	0	0	-0.377362	-0.380994	
1	1	0	0.094731	0.095830	
2	0	0	-0.049510	-0.049076	
0	0	1	-0.027912	-0.032524	
1	0	1	-0.001615	0.000423	
1	1	1	0.008920	0.009345	
0	0	2	0.001415	0.000151	
0	0	3	-0.000053	0.001201	
i	j	k	$t_{[i,j,k]}^{Nd/La}$		
0	0	0	1.594871	1.019156	
1	0	0	-0.470838	-0.068788	
1	1	0	-0.021513	-0.087446	
2	0	0	0.051356	0.021989	
0	0	1	-0.293301	-0.048961	
1	0	1	0.015698	-0.196251	
1	1	1	0.004019	-0.005498	
0	0	2	0.027121	-0.099677	
0	0	3	0.006169	-0.003715	
i	j	k	$t_{[i,j,k]}^{Nd/La-Ni}$		
0	0	0	0.000151	-0.011252	
1	0	0	-0.000239	0.009664	
1	1	0	-0.000037	0.003106	
2	0	0	-0.001777	0.001579	
0	0	1	-0.000157	-0.006010	
1	0	1	-0.007317	0.008403	
1	1	1	0.000070	0.006332	
0	0	2	0.000102	-0.004345	
0	0	3	-0.000040	-0.001681	

TABLE II. On-site energy and hopping parameters for two-orbital wannierization for $NdNiO^2$ and $LaNiO^2$.

- [11] M.-Y. Choi, K.-W. Lee, and W. E. Pickett, *Phys. Rev. B* **101**, 020503 (2020).
- [12] L. Si, W. Xiao, J. Kaufmann, J. M. Tomczak, Y. Lu, Z. Zhong, and K. Held, *Phys. Rev. Lett.* **124**, 166402 (2020).
- [13] S. Ryee, H. Yoon, T. J. Kim, M. Y. Jeong, and M. J. Han, *Phys. Rev. B* **101**, 064513 (2020).
- [14] S. Zeng, C. S. Tang, X. Yin, C. Li, M. Li, Z. Huang, J. Hu, W. Liu, G. J. Omar, H. Jami, Z. S. Lim, K. Han, D. Wan, P. Yang, S. J. Pennycook, A. T. S. Wee, and A. Ariando, *Phys. Rev. Lett.* **125**, 147003 (2020).
- [15] J. Krishna, H. LaBollita, A. O. Fumega, V. Pardo, and A. S. Botana, *Phys. Rev. B* **102**, 224506 (2020).
- [16] M. Osada, B. Y. Wang, K. Lee, D. Li, and H. Y. Hwang, *Phys. Rev. Materials* **4**, 121801 (2020).
- [17] Y. Cui, C. Li, Q. Li, X. Zhu, Z. Hu, Y. feng Yang, J. Zhang, R. Yu, H.-H. Wen, and W. Yu, *Chinese Physics Letters* **38**, 067401 (2021).
- [18] P. Jiang, L. Si, Z. Liao, and Z. Zhong, *Phys. Rev. B* **100**, 201106 (2019).
- [19] B.-X. Wang, H. Zheng, E. Kriviyakina, O. Chmaissem, P. P. Lopes, J. W. Lynn, L. C. Gallington, Y. Ren, S. Rosenkranz, J. F. Mitchell, and D. Phelan, *Phys. Rev. Materials* **4**, 084409 (2020).
- [20] D. Li, B. Y. Wang, K. Lee, S. P. Harvey, M. Osada, B. H. Goodge, L. F. Kourkoutis, and H. Y. Hwang, *Phys. Rev. Lett.* **125**, 027001 (2020).
- [21] K. Lee, B. H. Goodge, D. F. Li, M. Osada, B. Y. Wang, Y. Cui, L. F. Kourkoutis, and H. Y. Hwang, *APL MATERIALS* **8** (APR 1), 10.1063/5.0005103.
- [22] M. Osada, B. Y. Wang, B. H. Goodge, S. P. Harvey, K. H. Lee, D. F. Li, L. F. Kourkoutis, and H. Y. Hwang, *ADVANCED MATERIALS* **33** (NOV), 10.1002/adma.202104083.
- [23] S. W. Zeng, C. J. Li, L. E. Chow, Y. Cao, Z. T. Zhang, C. S. Tang, X. M. Yin, Z. S. Lim, J. X. Hu, P. Yang, and A. Ariando, “Superconductivity in infinite-layer lanthanide nickelates,” (2021), arXiv:2105.13492 [cond-mat.supr-con].
- [24] Q. Gu, Y. Li, S. Wan, H. Li, W. Guo, H. Yang, Q. Li, X. Zhu, X. Pan, Y. Nie, and H.-H. Wen, *Nature Communications* **11**, 6027 (2020).
- [25] M. Zhang, Y. Zhang, H. Guo, and F. Yang, *Chinese Physics B* **30**, 108204 (2021).
- [26] Y.-H. Zhang and A. Vishwanath, *Phys. Rev. Research* **2**, 023112 (2020).
- [27] P. Adhikary, S. Bandyopadhyay, T. Das, I. Dasgupta, and T. Saha-Dasgupta, *Phys. Rev. B* **102**, 100501 (2020).
- [28] X. Wu, D. Di Sante, T. Schwemmer, W. Hanke, H. Y. Hwang, S. Raghu, and R. Thomale, *Phys. Rev. B* **101**, 060504 (2020).
- [29] G.-M. Zhang, Y.-f. Yang, and F.-C. Zhang, *Phys. Rev. B* **101**, 020501 (2020).
- [30] C. Lu, L.-H. Hu, Y. Wang, F. Yang, and C. Wu, “Two-orbital model for possible superconductivity pairing mechanism in nickelates,” (2021), arXiv:2112.02610 [cond-mat.str-el].
- [31] H. Sakakibara, H. Usui, K. Suzuki, T. Kotani, H. Aoki, and K. Kuroki, *Phys. Rev. Lett.* **125**, 077003 (2020).
- [32] Z. Wang, G.-M. Zhang, Y.-f. Yang, and F.-C. Zhang, *Phys. Rev. B* **102**, 220501 (2020).
- [33] V. I. Anisimov, D. Bakhvalov, and T. M. Rice, *Phys. Rev. B* **59**, 7901 (1999).
- [34] K.-W. Lee and W. E. Pickett, *Phys. Rev. B* **70**, 165109 (2004).
- [35] A. S. Botana and M. R. Norman, *Phys. Rev. X* **10**, 011024 (2020).
- [36] E. Been, W.-S. Lee, H. Y. Hwang, Y. Cui, J. Zaanen, T. Devereaux, B. Moritz, and C. Jia, *Phys. Rev. X* **11**, 011050 (2021).
- [37] M. Jiang, M. Berciu, and G. A. Sawatzky, *Phys. Rev. Lett.* **124**, 207004 (2020).
- [38] Y. Nomura, M. Hirayama, T. Tadano, Y. Yoshimoto, K. Nakamura, and R. Arita, *Phys. Rev. B* **100**, 205138 (2019).
- [39] L.-H. Hu and C. Wu, *Phys. Rev. Research* **1**, 032046 (2019).
- [40] J. Karp, A. S. Botana, M. R. Norman, H. Park, M. Zingl, and A. Millis, *Phys. Rev. X* **10**, 021061 (2020).
- [41] F. Lechermann, *Phys. Rev. X* **10**, 041002 (2020).
- [42] R. Blankenbecler, D. J. Scalapino, and R. L. Sugar, *Phys. Rev. D* **24**, 2278 (1981).
- [43] T. Ma, F. Hu, Z. Huang, and H.-Q. Lin, *Applied Physics Letters* **97**, 112504 (2010).
- [44] T. Ma, H.-Q. Lin, and J. Hu, *Phys. Rev. Lett.* **110**, 107002 (2013).

- [45] H. Lu, M. Rossi, A. Nag, M. Osada, D. F. Li, K. Lee, B. Y. Wang, M. Garcia-Fernandez, S. Agrestini, Z. X. Shen, E. M. Been, B. Moritz, T. P. Devoreaux, J. Zaanen, H. Y. Hwang, K.-J. Zhou, and W. S. Lee, *Science* **373**, 213 (2021).
- [46] A. A. Mostofi, J. R. Yates, Y.-S. Lee, I. Souza, D. Vanderbilt, and N. Marzari, *Computer Physics Communications* **178**, 685 (2008).